Study on ultra-precision phase synchronization technique employing phase-locked loop*

ZHANG Wan-peng (张万鹏)**, WU Hong** (吴虹)****, ZHOU Wei-feng** (周卫锋)**, ZHAO Ying-xin** (赵迎新)**, LIU Zhi-yang** (刘之洋)**, and YANG Meng-huan** (杨梦焕)

Tianjin Key Laboratory of Optoelectronic Sensor and Sensing Network Technology, College of Electronic Information and Optical Engineering, Nankai University, Tianjin 300350, China

(Received 29 February 2020; Revised 21 April 2020)

Microwave-to-optical phase synchronization techniques have attracted growing research interests in recent years. Here, we demonstrate tight, real-time phase synchronization of an optical frequency comb to a rubidium atomic clock. A detailed mathematical model of the phase locking system is developed to optimize its built-in parameters. Based on the model, we fabricate a phase locking circuit with high integration. Once synchronized, the fractional frequency instability of the repetition rate agrees to 6.35×10^{-12} at 1 s and the standard deviation is 1.5 mHz, which indicates the phase synchronization system can implement high-precision stabilization. This integrated stable laser comb should enable a wide range of applications beyond the laboratory.

Document code: A **Article ID:** 1673-1905(2021)03-0134-6

DOI https://doi.org/10.1007/s11801-021-0036-3

Optical frequency combs are uniquely capable of phase coherently linking the optical, microwave, and terahertz regimes. Recently, Mode-locked fiber lasers (MLFLs) enable applications such as absolute distance measurements[1-3], frequency metrology[4] and long-distance time and frequency dissemination system[5-7]. Moreover, the application of optical frequency comb in the calibration of astronomical spectrometers has become a developing trend of planetary detection technology[8,9]. The crucial challenge for these applications is to generate ultra-high-stable pulses at a high repetition rate. The cavity length of MLFLs is easily influenced by various environmental factors such as temperature and pressure, which makes the repetition rate drift and the frequency stability deteriorate. Therefore, synchronizing a frequency comb to a more stable reference source is critical to the frequency stabilization of MLFLs[10]. Owing to their distinguished frequency stability, rubidium clocks are used as the frequency reference[11]. The repetition rate of the laser is about 80 MHz. It can be coarsely adjusted remotely. The repetition rate is phase-locked via feedback to the cavity length, which is controlled through a "slow" and a "fast" piezo-electric transducer (PZT) bonded to the intracavity fiber. A feedback loop is used to track a slight change in the repetition frequency. The jitter of the repetition rate can be quickly eliminated by changing the cavity length. Many schemes of the microwave-to-optical wave tight phase coherence based on the feedback loop have been proposed, such as the standard phase-locked loop (PLL) employing the analog phase detector[12,13], the PLL with the proportional-integral-derivative (PID) regulator[14], and fiber loop-based optical-microwave phase detector (FLOM-PD) based on Sagnac loop technique[6,15]. Among the various PLLs, charge pump PLL has become the mainstream in recent years, owing to the merit of integrated easily, low power, low jitter, the smallest zero capture phase error and a big capture scale. Here, we propose a highly integrated charge pump PLL system based on a phase-frequency detector (PFD) chip which possesses a programmable integer and fractional frequency synthesis to flexibly setup the frequency of the phase detector inputs. Although the FLOM-PD synchronous locking method can achieve microwave-to-optical phase synchronization with extremely high phase stability and low phase noise, it has a complex configuration and higher cost. Moreover, compared with the FLOM-PD method, the scheme we proposed possesses the characteristics of high anti-interference performance, compact structure, and simple installation and maintenance, which enable a wide range of applications beyond the laboratory.

As conceptually illustrated in Fig.1, a simplified configuration of a phase servo system consists of three basic configurations: phase detector (PD), loop filter (LP) and voltage controlled oscillator (VCO). Charge pump PLL is a typical representative of digital-analog mixed PLL, which has an excellent performance in phase tracking[16].

* This work has been supported by the National Natural Science Foundation of China (Nos.61571244 and 61871239), and the Tianjin Research Program of Application Foundation and Advanced Technology (No.18YFZCGX00480).
** E-mail: wuhong@nankai.edu.cn

Its PFD controls the charge-discharge time of the charge pump through the high and low levels of different duty cycles to reflect the phase error between the reference signal and the VCO. Its LP converts a current signal reflecting the phase error into a voltage signal and suppresses high-frequency components output by the PD and noise interference from the VCO. In our synchronization scheme, a voltage amplifier, a high-voltage driver, a piezo-electric transducer (PZT), and an MLFL make up the VCO of a charge-pump PLL. The real-time phase synchronization of the MLFL and the rubidium clock is guaranteed by continuously adjusting the scaling of the PZT. Additionally, we construct a mathematical model of phase locking system based on charge pump PLL for theoretical analysis. Theoretical analysis is conducive to the analysis of system performance and has guiding significance for further optimization design. For the convenience of analysis, the Laplace transform is used to transform the time-domain model of the phase locking system into a frequency-domain model. According to the mathematical model of each basic configuration of PLL, three important transfer functions are derived: open-loop transfer function, closed-loop transfer function, and error transfer function. We will analyze the final steady-state error, transient response and stability of the system through simulation to verify the feasibility of the phase locking scheme based on the charge pump PLL.

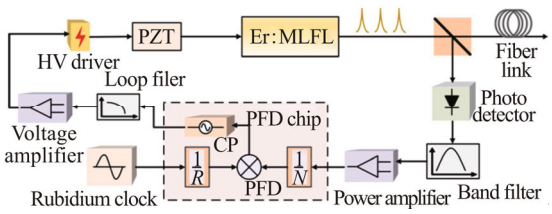

PFD: phase-frequency detector; CP: charge pump; HV: high-voltage; MLFL: mode-locked fiber laser; PZT: piezo-electric transducer

Fig.1 Configuration of the PLL utilized for phase locking of the mode-locked fiber laser

Fig.2 provides a mathematical model of mode-locked fiber laser for PLL technique in the frequency domain. $\Theta_i(s)$, $\Theta_o(s)$ and $\Theta_e(s)$ represent the Laplace transforms of the phase signals of the reference source, the laser, and the phase detector, respectively. Radiofrequency N counter allows a division ratio in the PLL feedback path. $I_{cp}(s)$ represents the s domain of the output signal of charge pump. $U_c(s)$ is the s domain representation of the output signal of the loop filter. K_d is the gain of the phase detector, $F(s)$ is the transfer function of the loop filter, and $K(s)$ is the transfer function of the VCO. From the model shown in Fig.2, three basic transfer functions of the PLL model in frequency domain, including open-loop transfer function $G(s)$, close-loop transfer function $H(s)$ and error-transfer function $H_e(s)$ are given by

$$G(s)=\frac{\Theta_o'(s)}{\Theta_e(s)}=\frac{K_dK(s)F(s)}{N}, \tag{1}$$

$$H(s)=\frac{\Theta_o'(s)}{\Theta_i(s)}=\frac{K_dK(s)F(s)}{N+K_dK(s)F(s)}, \tag{2}$$

$$H_e(s)=\frac{\Theta_e(s)}{\Theta_i(s)}=\frac{N}{N+K_dK(s)F(s)}. \tag{3}$$

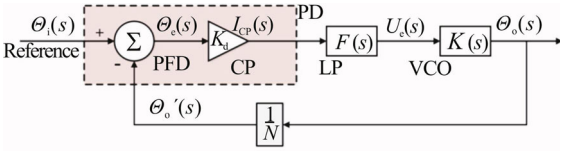

PFD: phase-frequency detector; CP: charge pump; PD: phase detector; LP: loop filter; VCO: voltage controlled oscillator

Fig.2 Mathematical model for PLL technique in the frequency domain

In the following, we will analyze the phase transmission characteristics of the phase detector, loop filter, and VCO to derive a detailed mathematical model of the phase locking system. A phase detector is a device whose output is proportional to the phase difference between the two input signals. The error signal $I_{cp}(s)$ can be expressed as

$$I_{cp}(s)=K_d\Theta_e(s)=K_d(\Theta_i(s)-\Theta_o'(s)), \tag{4}$$

where $\Theta_o'(s)$ is the phase arguments of mode-locked laser through the N frequency counter. K_d is the gain of the phase detector. Assuming that I_{cp} is the discharge current of charge pump, according to Eq.(4), the gain of phase detector of charge pump PLL can be expressed as

$$K_d=\frac{I_{CP}}{2\pi}. \tag{5}$$

The phase detector signal is composed of several items, and a post-stage loop filter is required to suppress its high frequency components and extract the phase error signal.

Fig.3 shows a commonly used active lead-lag filter. A lead-lag filter combines a phase-leading with a phase-lagging network. According to Thevenin's theorem, this circuit is applied to the filter loop of a charge pump PLL. Its transfer function $F(s)$ is given by

$$F(s)=\frac{A(1+s\tau_1)}{s^2\tau_2(\tau_0+\tau_1)+s(\tau_0+\tau_1+\tau_2)+1}, \tag{6}$$

where $\tau_0=R_0C_1$, $\tau_1=R_1C_1$, $\tau_2=R_2C_2$ and $A=R_0R_f/R_b$.

In the PLL locked state, the loop filter output is a regulated signal that reflects the phase error. The cavity length of the laser can be regulated by PZT driven voltage. The expansion and contraction of the laser resonator can compensate for phase jitter. Assuming the original cavity length is L_0, ignoring the effect of laser delay, the transfer function of VCO is given approximately by

$$K(s)\approx\frac{2\pi ck_o}{sL_0^2}, \tag{7}$$

where c is light velocity, and k_o is called VCO gain[13]. This equation is a first-order time-delay system of the standard VCO model. According to Eqs.(1)—(3) and Eqs.(5)—(7), open-loop transfer function and error-transfer function can be rewritten as

$$G(s)=\frac{AI_{CP}ck_0(s\tau_1+1)}{L_0^{\ 2}Ns(s^2\tau_2\tau'+s\tau+1)}, \tag{8}$$

$$H_e(s)=\frac{s^3\tau_2\tau'+s^2\tau+s}{s^3\tau_2\tau'+s^2\tau+\frac{sAI_{CP}ck_0\tau_1}{NL_0^{\ 2}}+s+\frac{AI_{CP}ck_0}{NL_0^{\ 2}}}, \tag{9}$$

where $\tau_0=\tau_0+\tau_1+\tau_2$ and $\tau'=\tau_0+\tau_1$. τ and τ' are the time constants of the loop filter. In the following, we will apply Eqs.(8) and (9) to analyze the characteristic of the PLL.

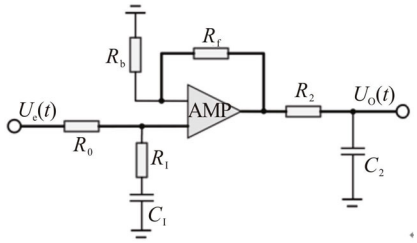

Fig.3 Schematic of low-pass filter for PLL

In engineering control systems, the final steady-state error is defined as the deviation between the expected value and the actual value after the transient response has died out[17]. In a PLL system, the final steady-state error is considered to be the phase error $\theta_e(\infty)$. To see how the phase locking system settles on typical excitation signals applied to its reference input, we will derive the final steady-state errors for phase steps, frequency steps, and frequency ramps. When the excitation signal $\theta_i(t)$ is given, the phase error $\theta_e(t)$ is calculated by the final phase error $H_e(s)$ as defined in Eq.(9). Using the final value theorem of the Laplace transform, $\theta_e(\infty)$ is written as

$$\theta_e(\infty)=\lim_{s\to0}s\Theta_e(s)=\lim_{s\to0}s\Theta_i(s)H_e(s). \tag{10}$$

If a phase step of size $\Delta\Phi$ is applied to the excitation, we have $\Theta_i(s)=\Delta\Phi/s$. Using Eqs.(9) and (10), the steady-state error is given by

$$\theta_e(\infty)==\lim_{s\to0}s\frac{\Delta\Phi}{s}H_e(s)=0. \tag{11}$$

This quantity becomes 0. According to Eq.(11), when the PLL system operates in steady-state, the system can offset the phase difference jitter between the reference source and the laser. In case of frequency step of size $\Delta\omega$, for its Laplace transform we get $\Theta_i(s)=\Delta\omega/s^2$. Hence, the steady-state error becomes

$$\theta_e(\infty)==\lim_{s\to0}s\frac{\Delta\omega}{s^2}H_e(s)=\frac{\Delta\omega NL_0^{\ 2}}{AI_{CP}ck_0}. \tag{12}$$

This quantity becomes a constant. According to Eq.(12), when the PLL system is in steady-state, the phase difference between reference and laser is constant. For the Laplace transform of the frequency ramp, we have $\Theta_i(s)=\Delta\omega'/s^3$ where $\Delta\omega'$ is the derivative of $\Delta\omega$. For the steady-state error we get

$$\theta_e(\infty)==\lim_{s\to0}s\frac{\Delta\omega'}{s^3}H_e(s)\neq\text{constant}. \tag{13}$$

According to Eq.(13), the final steady-state error does not approach a constant. Hence, the laser cannot synchronize phase with the reference source. In the phase locking system, selecting a high-precision long-term stable atomic clock as a reference is equivalent to a frequency step of size $\Delta\omega$ as a reference input. Therefore, the final steady-state error of the control system is constant, and the laser maintains phase stability. Generally, when the response rate of the phase locking system is too slow, the system is prone to instability. Therefore, it is critical to analyze the transient response of the phase locking system.

Transient response is defined as the response process from the initial input to the final steady state. Knowing the final phase error $H_e(s)$ of PLL, we can calculate its response on important excitation signals, including phase steps, frequency steps, and frequency ramps. For the convenience of simulation analysis, we define the default values of the parameters. We assume the repetition rate of MLFLs is 80.011 4 MHz, and the charge pump output maximum current is 5 mA. Under this condition, τ_0 is 3×10^{-9}, τ_1 is 3.3×10^{-10}, τ_2 is 1×10^{-6}, A is 600, k_0 is 1.3×10^{-4}, and L_0 is c/80 011 400, where c is light velocity. Fig.4(a) shows the transient response of the phase-locking system to a phase step. It can be seen in Fig.4(a) that when the phase changes abruptly, the system can quickly eliminate the phase error and recover to a steady state. If a frequency ramp is applied to the reference input, the transient response of the phase-locking system is shown in Fig.4(b). In this case, the phase error increases with the passage of time, and the system cannot get into a steady state.

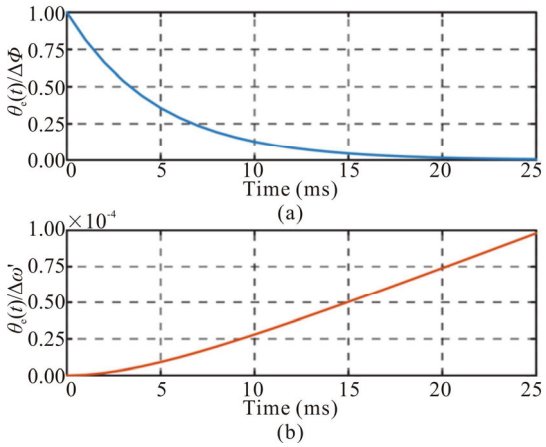

Fig.4 Transient responses of the phase-locking system to (a) a phase step and (b) a frequency ramp

Here, the frequency step signal output by the rubidium clock is used as the reference excitation source in phase locking system. Therefore, we should focus more on the influence of parameters on the transient response when the frequency step signal is applied to reference input. The designer can adjust different parameters for acquiring different transient response in order to optimize the built-in parameters. According to Eq.(9), VCO gain

coefficient k_0 and frequency counter N have opposite effects on the transient response of the system. In this article, we only adjust the parameter N. As shown in Fig.5(a), our phase locking system has an automatic adjustment function that guarantees the phase synchronization of the laser and the rubidium clock. According to the theory of femtosecond oscillator noise analysis, the higher harmonics of the repetition frequency carry more phase noise information[18]. For this reason, directly synchronizing the higher harmonics of the repetition frequency means that more phase noise can be suppressed. Decreasing the frequency N counter can shorten the time for the transient response to reach the steady state, and improve the synchronization accuracy as shown in Fig.5(b).

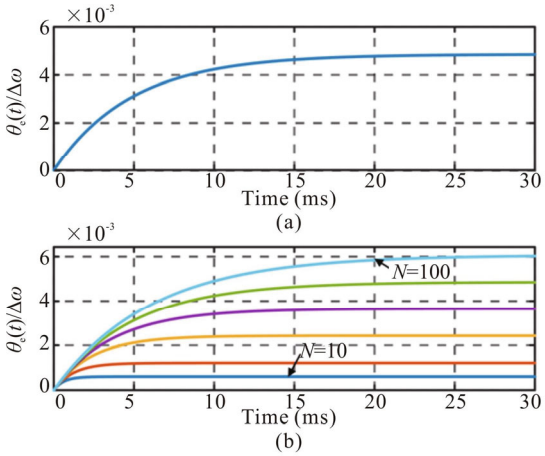

Fig.5 Transient responses of the phase-locking system to (a) a frequency step and (b) the frequency step with different *N*

The degree of stability is a crucial characteristic of the PLL. It indicates the ability of the loop to maintain system balance under external interference, noise, and other factors. The stability criterion has presented that a PLL with a positive phase margin is stable, otherwise, it is unstable. Assuming $\omega=\omega_0$ and $|G(j\omega)|=1$, phase margin is defined as $\mathrm{Arg}[G(j\omega)+\pi]$. In engineering applications, the phase margin is not less than 45°. The larger the phase margin, the more stable the system, but the more obvious the damping. The Bode plot is a useful method for evaluating closed-loop stability by using the characteristics of open-loop frequency transmission. It is an effective tool for characterizing stability. According to Eq.(8), we can draw the Bode plot of the system. Fig.6 shows Bode plot of the phase locking system of the MLFL. The phase margin is greater than 45°, and the system is in a stable state. The response bandwidth of the phase locking system is limited by the PZT bandwidth of the laser, which generally does not exceed 10 kHz.

In the following, we deploy a detailed experimental system and fabricate a phase locking circuit with high integration based on the phase-locking theoretical analysis of the mode-locked laser. The frequency stability characteristics of the system are measured experimentally to verify the feasibility of the phase locking system. Fig.7 shows the schematic diagram of the experimental setup of the phase-locking system. In our experiment, the rubidium clock is utilized as the reference. Meanwhile, the collimated pulse beam passes through the photodetector to produce the microwave signal to be synchronized. Our homemade PLL device selects the PFD chip(ADF4155). This chip allows the implementation of fractional or integer N PLL frequency synthesizers. Moreover, this chip is for use with the repetition rate of MLFL up to an 8 GHz operating range. Direct digital frequency synthesizer (DDS) produces signals with different phases and frequencies used to verify the final steady-state error and transient response of the phase locking system. A microcontroller unit (MCU) controls all on-chip registers through a 3-wire interface. Meanwhile, the MCU monitors the phase locked state of the system by sampling the output voltage of the loop filter. The band-pass filter (BPF) uses K&L microwave C series 5C40-800/U20-O/O narrow-band filter, which has the features of high Q value, low insertion loss, and high out-of-band rejection.

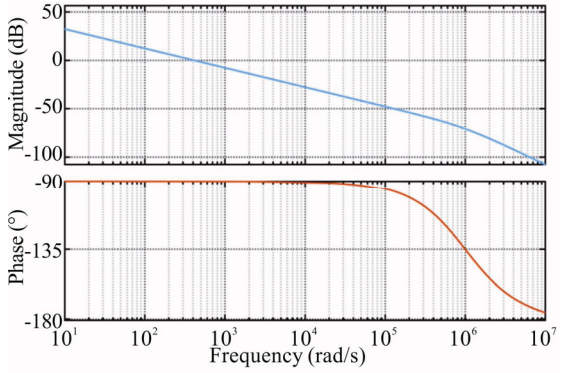

Fig.6 Bode plot of the phase locking system

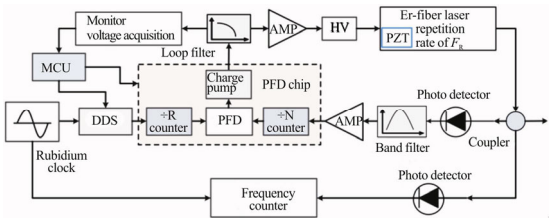

MCU: microcontroller unit; PFD: phase-frequency detector; HV: high-voltage; PZT: piezo-electric transducer

Fig.7 Schematic diagram of the experimental setup

The mode-locked laser produces an optical pulse with a repetition rate of 80.011 4 MHz. The optical pulse is divided into two channels by a beam splitter. One channel is used to synchronize with the reference, and the other channel is input to the frequency counter for evaluation of phase-locking performance. The repetition frequency is measured by the Agilent 53230A frequency counter that offers resolution capabilities up to 12 digits/sec frequency resolution on a one second gate and single-shot time

interval measurements down to 20 psec. The MLFL is not equipped with anti-vibration and temperature control devices in the experimental test. The sampling interval of the frequency counter is set to 0.1 s. Under the above conditions, Fig.8 shows the value of the repetition rate of the MLFL in the open-loop state and the locked state for one hour. In the open-loop state, the standard deviation of frequency jitters is 16.716 5 Hz. Meanwhile, in the locked state, the standard deviation of frequency jitters is 1.5 mHz. By comparison, the phase-locking performance is exceptionally outstanding, and the standard deviation can be improved by four orders of magnitude. Generally, frequency instability is an effective tool for characterizing the phase locking performance of lasers. It is defined as a random fluctuation of the average frequency due to noise modulation. It reflects the degree of frequency instability and is usually expressed as Allan variance[19]. Fig.9 shows the frequency instability of the MLFL in the locked and open-loop states and the frequency instability of the rubidium clock. Experimental results show that the frequency instability can reach 6.35×10^{-12} at 1 s in the locked state, and the frequency instability is improved by two orders of magnitude. The experimental results prove that our proposed phase locking system can achieve high-precision phase synchronization of the MLFL and the rubidium clock.

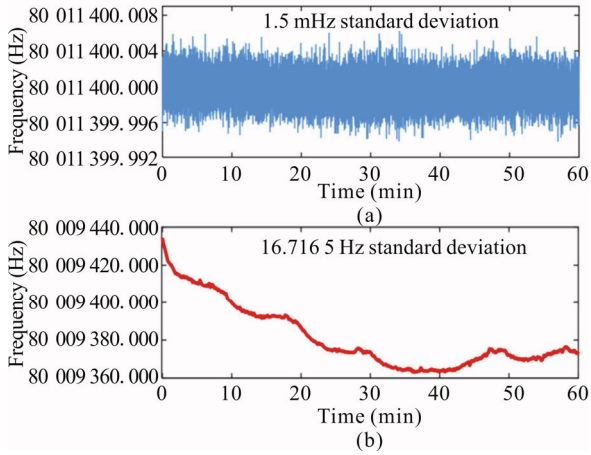

Fig.8 Repetition rates of the MLFL in (a) the locked state and (b) the open-loop state

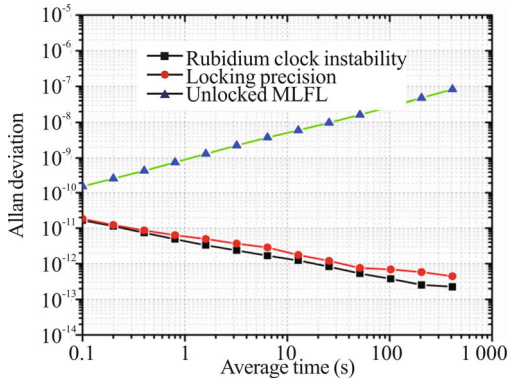

Fig.9 Measurement of the fractional frequency instability

We report the phase synchronization technique of the MLFL to the rubidium clock with a highly integrated charge pump PLL system. By setting up a mathematical model of the phase locking system, we build an experimental phase locking system. The simulation and experimental results jointly prove out the correction of our model. With the system described above, the frequency comb is tightly locked in the rubidium clock. For further optimization, we will set out to improve the phase-detection frequency, utilize a more accurate atomic clock, and set up a temperature-control and shock-proof device for the laser to ensure more accurate phase synchronization in the further work. Our proposed phase locking system is anticipated to be applied in various scientific as well as engineering areas. Optical frequency combs allow for high-fidelity frequency transfer to the mid-infrared, terahertz, and microwave domains. Time and frequency communication is achieved by comparing counter-propagating optical pulse trains from optical frequency combs stabilized to clocks at remote locations. Hence, the technique of microwave-to-optical wave tight phase coherence is the prerequisite for microwave communications via fiber link and future precise navigation and sensing systems. Also, this technique could similarly enable applications such as precise formation flying of phased satellite arrays.

References

[1] Trocha P, Karpov M, Ganin D, Pfeiffer MHP, Kordts A, Wolf S, Krockenberger J, Marin-Palomo P, Weimann C, Randel S, Freude W, Kippenberg TJ and Koos C, Science **359**, 887 (2018).

[2] Wang Guo-chao, Tan Li-long and Yan Shu-hua, Sensors **18**, 500 (2018).

[3] Coddington I, Swann W C, Nenadovic L and Newbury N R, Nature Photonics **3**, 351 (2009).

[4] Oliver Kliebisch, Dirk C. Heinecke, Stefano Barbieri, Giorgio Santarelli, Hua Li, Carlo Sirtori and Thomas Dekorsy, Optica **5**, 1431 (2018).

[5] Chen Xing, Shang Jian-ming, Wang Dong-xing, Ci Cheng, Zhang Wan-peng, Liu Bo, Wu Hong, Yu Song and Zhang Zhi-gang, CLEO: Applications and Technology, Optical Society of America, JW2A.152 (2018).

[6] Kwangyun Jung, Junho Shin, Jinho Kang, Stephan Hunziker, Chang-Ki Min and Jungwon Kim, Optics Letters **39**, 1577 (2014).

[7] CI Cheng, Wu Hong, Tang Ran, Liu Bo, Chen Xing, Zhang Xue-song, Zhang Yu and Zhao Ying-xin, Optoelectronics Letters **14**, 109 (2018).

[8] Ronald Holzwarth, Rafael A. Probst, Tilo Steinmetz, Yuanje Wu, Thomas Udem and Theodor W. Hänsch, CLEO: Science and Innovations, Optical Society of America, STh4H.3 (2016).

[9] E. Obrzud, M. Rainer, A. Harutyunyan, M.H. Anderson, J. Liu, M. Geiselmann, B. Chazelas, S. Kundermann, S.

Lecomte, M. Cecconi and A. Ghedina, 2018 European Conference on Optical Communication (ECOC), IEEE (2018).

[10] Cundiff, Steven T. and Jun Ye, Journal of Modern Optics **52**, 201 (2005).

[11] Micalizio S, Godone A, Calosso C, Levi F, Affolderbach C and Gruet F, IEEE Transactions on Ultrasonics Ferroelectrics & Frequency Control **59**, 457 (2012).

[12] Brian R. Washburn, Scott A. Diddams, Nathan R. Newbury, Jeffrey W. Nicholson, Man F. Yan and Carsten G. Jørgensen, Optics Letters **29**, 250 (2004).

[13] Hou Dong, Ning Bo, Li Peng, Zhang Zhi-gang and Zhao Jian-ye, IEEE Journal of Quantum Electronics **47**, 891 (2011).

[14] Hou Dong, Wu Jiu-tao, Ren Quan-sheng and Zhao Jian-ye, IEEE Journal of Quantum Electronics **48**, 839 (2012).

[15] Kwangyun Jung, Junho Shin and Jungwon Kim, IEEE Photonics Journal **5**, 5500906 (2013).

[16] Hanumolu P. K., Brownlee M., Mayaram K. and Moon, IEEE Transactions on Circuits & Systems I Regular Papers **51**, 1665 (2004).

[17] R. E. Best, McGraw-Hill Education, 2007.

[18] X. Shan and D. M. Spirit, Electronics Letters **29**, 979 (1993).

[19] Richard G. Wiley, IEEE Transactions on Instrumentation and Measurement **26**, 38 (1977).